

Author's Signature: _____

Contents

1. Introduction 1

2. Methodology 2

2.1 Goals 4

2.1.1 Short term ...4

2.1.2 Long term 4

3. Plan 4

3.1 Mechanism 5

3.2 Statistics 5

4. Impact 7

5. Metrics 8

6. Conclusion 10

References 11

Bibliography 12

List of Figures

1 Block diagram of Collection and Reporting Mechanism. 6

2 Sample plot from query engine. 9

1. Introduction

AFS (originally, Andrew File System) is a widely-deployed, mature, field-proven distributed file system product used by companies, universities, and laboratories world-wide. However, it is not trivial to operate: running an AFS cell is a formidable task. It requires a team of dedicated and experienced system administrators who must manage a user base numbering in the thousands, rather than the smaller range of 10 to 500 faced by the typical system administrator. For institutions such as JPL, which do not have the motivation or funding to pay for dedicated AFS programmers, researchers, and source code access like University of Michigan, Carnegie-Mellon University (CMU), or MIT, the task can be daunting. Transarc supplies the base product, training classes, and some technical support, but in-house engineering is necessary to deploy and maintain AFS as the installation changes and grows. The requisite engineering is dependent on the characteristics of a given site: available server hardware, the average user profile, user/group needs, administrative staff size, network topology and network capacities. In particular, a rapidly growing distributed computing infrastructure, such as that at JPL, needs to be constantly monitored to continue to provide adequate, reliable service. The goal of this thesis is to develop a thorough set of integrated metrics that quantify the activity of an AFS site. This information should provide timely, practical, essential information to system architects, programmers, administrators, and managers.

The main focus of the metrics will be monitoring growth and bottlenecks, to answer such questions as:

- How much is server disk usage increasing, and which volumes?
- How much fileserver- network traffic is occurring?
- What I/O bandwidth are the servers achieving, and are they ever running at capacity?
- Are *any* resources being used to capacity, and due to what usage patterns?
- Which software supplied out of AFS is being used most often, and deserving of support?

The two main thrusts of metrics collection are (1) the extrapolation of measurements to predict resource exhaustion, and (2) the isolation of bottlenecks so that more resources can be devoted to widen the path. For example, it may become apparent that a certain server subnetwork is saturated; based on the individual traffic from each server, it may be appropriate to upgrade network hardware or split the servers onto different subnets.

While users often complain about network performance, making statements like: "I wonder why it's taking so long to do backups" or "Access to my account seems slow over the past few days", these complaints of inadequacies are only symptoms and rarely, without some additional "hard" data, lead to the true cause(s) of the poor network performance. The specific information necessary for intelligent maintenance cannot be derived from such anecdotal reports. For example, is sluggish file access due to a clogged network or a server disk I/O problem? Monitoring file servers and networks is necessary.

In summary, accurate performance data are necessary for the efficient maintenance of a complex distributed service such as AFS, especially for the anticipation of performance problems and for the rational justification of expenditures.

2. Methodology

Such a study may seem unnecessary at first glance; after all, successful installations have existed ranging up to 30,000 users for years now in universities such as MIT, University of Michigan, Stanford, CMU, as well as major financial and technology companies such as IBM. However, making AFS work at large places like these does not happen all by itself. One must consider that AFS's success at an enormous place like University of Michigan is due to the extraordinary talents of a dedicated team of system programmers, researchers, and administrators working closely with Transarc and the full source code. Based on detailed monitoring efforts, these teams wrote performance enhancements and design fixes, some of which were folded back into the commercial Transarc source. Having a high level of access to AFS internals allowed them to tweak architecture and performance as necessary. For example, Peter Honeyman explored intermediate caching servers to reduce server load [Hone 92], and developed enhancements to the Rx code to vastly improve its performance over slow links. While all customers now benefit from these fixes and enhancements, most customers (including JPL) are ill-equipped, without an integrated set of tools, to detect future bottlenecks, barriers, and bugs.

Another major difference between JPL and those institutions is that there is no research aspect to the file service itself; JPL's File Service staff is small and JPL's scientists are concerned with other types of research. MIT's Project Athena and the Center for Information and Technology Integration (CITI) at University of Michigan, while providing an essential service to the campus population, are both experimental and research-oriented by nature. Failures are more tolerable because data are rarely mission critical, as is often the case at JPL. Administrators at sites like JPL must benefit from the conservative strategy of staying safely ahead of the demand curve and preempting as many problems as is economically and rationally justifiable.

One might still argue that most failures will be due to unpredictable circumstances, such as the bizarre interactions that caused the athena. init. edu cell to meltdown several times in 1994. I refute that by identifying a new class of resource exhaustion failures.

The user profile at JPL is different from that of huge university sites. While the quota at MIT is currently 12.5MB (considered high for a university), almost all user quotas at JPL are at least 100 MB, and active users or users of large programs (such as myself) have quotas of at least 200MB. The profile differs in other significant ways. Many of JPL's users use personal PCs and Macintoshes, not UNIX workstations. These machines have a very different usage profile: Macintosh and PC files typically contain monolithic data structures representing complex graphics and formatted text, for example an entire newsletter, slide presentation, or spreadsheet. The traditional file size distribution observed in well-known previous studies, that very small files account for 90% of the total [Ousterhout 85], may not be true in this newly heterogeneous environment. In addition, the follow-up study on the original BSD filesystem study [Baker 91] showed that the largest files, while still accounting for only 10% in quantity, had increased in size by an order of magnitude and thus dominated the byte count. Thus it is reasonable to suspect new, unpredictable problems will arise from a preponderance of large files.

Macintosh and Windows users rely on protocol translators (themselves AFS clients) to emulate AFS services over a special protocol layered on TCP/IP or an AppleTalk LAN. This is another major issue of concern since load from potentially hundreds of personal computers will have to filter through these

translators. This load needs to be carefully monitored as well. Little of my literature research has turned up information about evaluating or monitoring protocol translators.

The above, combined with the generally accepted knowledge that network usage grows exponentially as it becomes more available to users (via such services like AFS and the Web) there is reason to be concerned about growth at any deployment where the network and a client/server model is being used for something as critical as a shared file system. JPL is at exactly that stage where many users, many of them used to older, smaller-scale systems, are just beginning to “warm up” to a distributed computing environment. Currently about 15% (900 out of 6000) of the lab’s personnel have AFS accounts, and preliminary statistics show only about 20% of them are truly active. The Enterprise Information Systems (EIS) project, which manages the AFS cell, intends to eventually have everyone on lab using it so they may benefit from a shared, secure, centrally managed file space. It is important to have set of thorough metrics and diagnostics in place before this happens.

Since there are obviously valid concerns, one might suspect tools to monitor these types of loads already exist. In fact, they do, and I have found a number in my current research: tcpdump [Mcca], the Andrew Benchmark [Saty], afsmon [Neer], and sentinel [Wong] from CMU, sdi¹ from MIT, perfimeter, iostat, and vmstat² from Sun, and bos, vos, afsmonitor, rxdebug, udebug, and scout from Transarc Corporation itself. While each of these tools is capable of collecting detailed statistics of a particular type, there is no architecture to cleanly integrate them yet. In particular, these tools need to be integrated or rewritten to collect the needed types of data from a number of servers and protocol translators, store them in a common format, and do so automatically at regular intervals, without needing monitoring themselves by humans. Further, it is necessary to generate warnings which can be sent to pagers and e-mail accounts of the system administrators. Finally, the data needs to be graphed and summarized to be made accessible to human inspection.

Essentially, there are many tools out there, but they don’t work together, and don’t provide the types of useful summary information that let humans know what the data really means. Therefore, a truly integrated set of metrics is much more useful than all the above tools combined. Managers need justification to spend money on a project and need to see results. An attractive set of labelled graphs, perhaps available on the Web and containing up-to-the-minute information, will show unequivocally how much the file service is being used and stressed. If the usage is growing, as it is at JPL, it will clearly pinpoint the need for new hardware and staff (which is the case at JPL) and some indication of how much of each.

This project concentrates on AFS as the production environment and DFS as the next generation. Transarc wants to promote their next-generation product, DFS, as an integrated part of their implementation of Open Software Foundation’s Distributed Computing Environment (DCE). To adapt the work of this thesis, all that is necessary is to adapt some of the specific data collection methods to the internals of DCE and DFS. The overall architecture remains the same, especially since DFS is so closely based on AFS. In addition, the data collection and analysis tools I am constructing are easily general enough to be applied to any other network-based service.

¹written by **Athena operations staff** members Matt Braun (mhbraun@mit.edu), Mike Whitson (mwhitson@mit.edu), and David Krikorian (dkk@mit.edu)

²part of the standard Solaris 2.x distribution from Sun Microsystems, Inc.

2.1 Goals

2.1.1 Short term

The goals of this thesis are as follows.

• **1S.** Create a data-collection and database engine to absorb large amounts of performance data and provide highly configurable graphs and summaries of selected data. On top of this will be layered a flexible query interface accessible via the Web. This tool will be the vehicle for the following.

• **2S.** Raise alarms when any resource gets dangerously close to exhaustion: especially partition usage. since this is a “hard” failure

Partition usage deserves some elaboration here. It will be very valuable to administrators³ to know which partitions are filling up fastest and which ones are near full, so they may move volumes around and know where to create new ones. Thus detailed reporting capability will be made available in this regard.

• **3S.** Identify bottlenecks by looking for clipping: on the network, on the server’s disk, CPU, or protocol limitations

• **4S.** Provide a operator-console interface, probably on the Web, to display super-high-level summary of cell status

2.1.2 Long term

• **1L.** Provide curve-fitting mechanisms that will try to predict various classes of resource exhaustion: server CPU, memory, disk capacity, disk I/O, network

• **2L.** Aid the cell engineers in identifying common failure modes by providing a summary of logged failures, and the values of important parameters at time of failure: server CPU and I/O loading, network load, time of day, and possibly other metrics.

• **3L.** Identify usage patterns on shared software volumes. This can be used so administrators and tool builders know where to focus their support.

3. Plan

Presented here is a description of the core database mechanism used to manage the data, followed by the specific statistical data that will be inserted into the database to meet the goals.

³from personal conversations with cognizant administrators here at JPL and Bill Cattey at MIT

3.1 Mechanism

The data-collection and database engine have already been written. Currently, sets of data can be requested and retrieved via any set of properties. I am implementing the routines to process the data into human-digestible forms. I have formulated a number of simple, elegant operations to massage the data in many different ways depending on the perspective desired. I then plan to create a simple path for the data to flow from the query engine to a plotting program (gnuplot) to the Web. For example, it will be possible to request the histogram seen in the Metrics section, or a line graph of the most traffic-intensive hour of each day, or a line graph of total disk usage over the past month, or a sorted tally of the most-accessed volumes.

Figure 1 clarifies the entire collection and reporting mechanism.

3.2 Statistics

I plan to monitor the following statistics, for which I will explain how they can be aggregated to meet the above goals. Each set of statistics is labelled the same as the goal it fulfills.

- 2S. There are several metrics that need to be monitored for this goal, one for each class of resource exhaustion.

Partition usage: This will be monitored at two levels: frequent monitoring due to the severe nature of an associated failure, and daily summaries for long-term predictions.

Partition overrun is important to monitor because it is common practice to oversubscribe partition space, on the assumption that most users will use significantly less than their quota. I plan to monitor the free bytes on every AFS partition in the cell (a total of about 100 on 5 machines currently, but growing) every five minutes, assuming this does not present any noticeable extra load. If a condition that is suspicious (rapidly filling partition) or an emergency (partition out of space) arises, the logging software will short-circuit the path through the database and send e-mail/pager warnings to cognizant administrators. At this point, the volume(s) which are filling up the partition can be searched out and locked by the software until an administrator can investigate the problem.

To accomplish daily monitoring, a fixed time-of-day sample can be simply be chosen from the frequent samplings and pushed into the database for long-term storage and analysis.

Server subnet usage: Either the hub or the logging machine needs to be queried for aggregate traffic totals. I plan to sample these totals every several minutes. This can then be processed by the query engine to easily pick out long-term trends, like peaking at certain times of day or long term average increase.

Server queue length: I plan to run `rxdebug` queries approximately every 15 minutes to monitor the number of active requests. If this length gets too long, the server can no longer process requests, an indication more servers may be needed, or the server needs upgrading.

Server and protocol translator load: I plan to run several system diagnostic utilities (`uptime`, `iostat`, `vmstat`) every 15 minutes or thereabouts on each machine to see if the demand for the CPU and

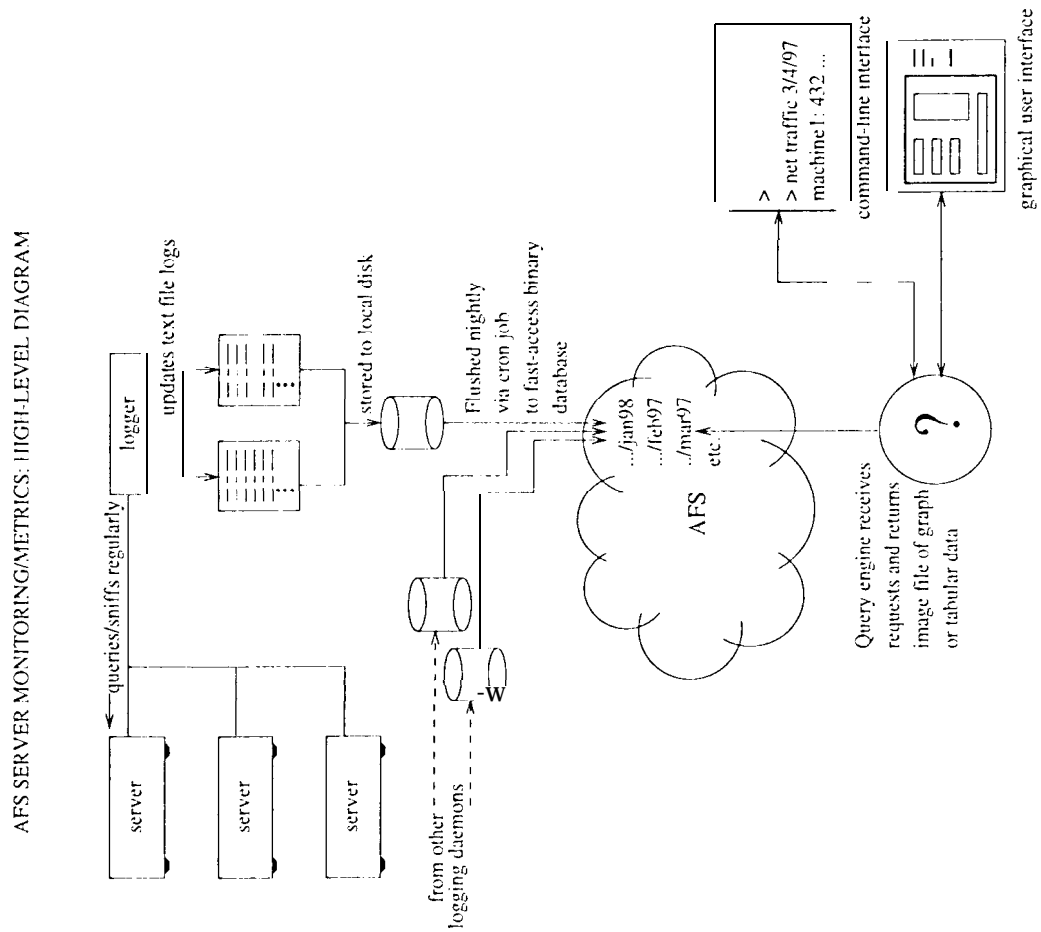


Figure 1: Block Diagram of Collection and Reporting Mechanism.

— Periodic server querying via system diagnostic utilities.

Each utility takes between several milliseconds and a second to execute. They will run with a frequency on the order of four times per hour, and thus clearly have minimal impact.

Frequent partition monitoring via `vos partinfo`.

This is very similar to the above, except running on the order of 12 times per hour. Noticeable impact is remotely possible (this itself can be monitored by connection queue length), and if so, it can be throttled back to query less often.

-- Daily server querying via `vos suite`.

AFS provides various `vos` (VOLUME Server) commands (`vos examine`, for example) to obtain detailed volume-oriented information. Because this data is only needed once a day, it can be done during the period of least user activity (early in the AM). The logging machine will capture this data as well.

- Passive network monitoring.

Finally, the logging machine will sniff the server subnet and capture all AFS-related packets. Timing, bandwidth, and port-oriented data is collected this way. The only impact on any other part of the system is that the switched hub must echo traffic from the AFS servers to this machine, but the hub is easily capable of this without its own performance being affected.

Thus, extensive statistics can be gathered without noticeably impacting the rest of the system. Collection involves appropriate periodic and passive mechanisms, as well as leaving as much of the processing as possible to a dedicated logging machine. Again see figure 1 for the logging architecture.

5. Metrics

Figure 2 shows a possible output of the query engine. A user might request all data from Oct 7 to November 20, on all machines, that relate to “FetchData” and “StoreData” requests. This might be used to examine the daily cycle pattern (which hours tend to be busiest), what the highest peaks are, and if there appears to be a general trend of increasing traffic. More specifically, a cell engineer would know to monitor the hours from 2 to 4 more closely to catch the peak usages of the system resources. This is a good metric because the fetch and store operations, byte-wise, are the heaviest weight operations of all AFS transactions for the simple reason that is the main end-service a distributed file system provides. Thus it is a good metric to examine, as a first-order approximation, the load presented to the file servers and the network by the users.

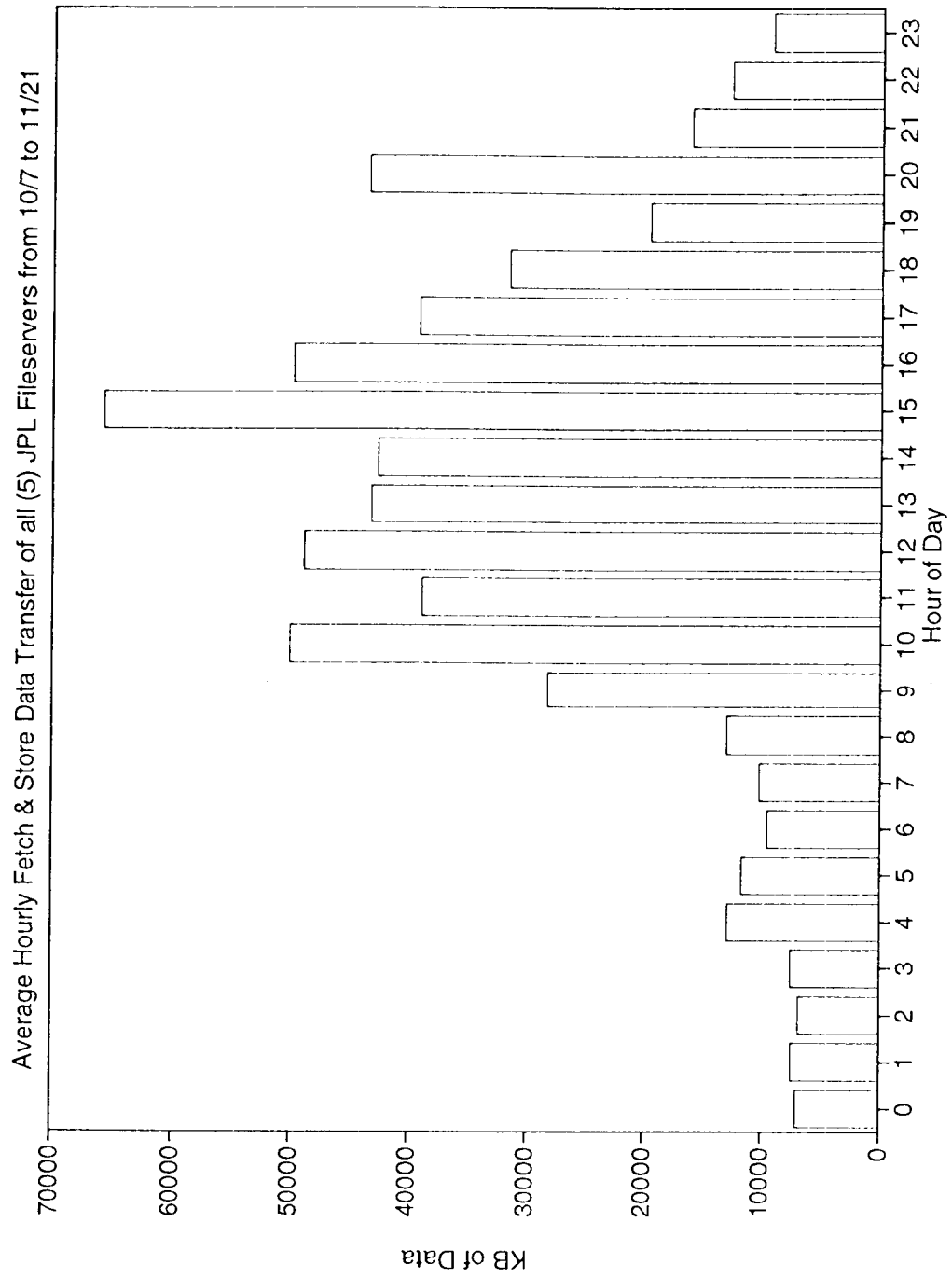


Figure 2: Sample Plot from Query Engine.

6. Conclusion

This thesis will examine issues at a higher level than the day-to-day administration of an AFS cell. Its goal is to develop metrics and long term look-ahead strategies that ensure that an AFS installation (and in general any distributed file system installation, such as DFS) will remain available and keep up with demand in a proactive management approach.

References

[Bake 91] **Baker**, Mary **G.**, Hartman, John H., Kupfer, Michael D., Shirriff, Ken W., Ousterhout John K., *Measurements of a Distributed File System*. Proceedings of the 13th ACM Symposium on Operating System Principles, University of California, Berkeley, CA July 1991.

[Hone 92] P. Honeyman D.A. Muntz, *Multilevel Caching in Distributed File Systems*. Proceedings of the Winter USENIX Conf., San Francisco, CA, January 1992.

[Mcca] Available via anonymous ftp from ftp.ee.lbl.gov as tcpdump.tar.Z. Information available on the tcpdump@ee.lbl.gov mailing list. Written by Van Jacobson, Steve McCanne, and Craig Leres. Copyright ©1988-1990 The Regents of the University of California.

[Neer] Neergard, Pete (jpn@cmu.edu) Distribution, site unknown.

[Oust 85] Ousterhout, J. K., DaCosta, H., Harrison, D., Kunze, J. A., Kupfer, M. Thompson. J. G., *A Trace-Driven Analysis of the UNIX 4.2 BSD File System*. Proceeding of the 10th Symposium on operating System Principles, Orcas Island, WA, December 1985, pp 15-24.

[Saty] A good citation appears in *Scale and Performance in a Distributed File System*. Howard, J. H., Kazar, M.L., Menees, S. G., Nichols, D.A., Satyanarayanan, M., Sidebotham, R. N., West, M.J. ACM Transactions on Computer Systems, 6(1), February 1988.

[Wong] Wong, Walter, wally+@cmu.edu. Distribution can be found in
`/afs/transarc.com/public/afs-contrib/tools/sentinel`

Bibliography

Mena III, A. Burnett, C. *Performance characteristics of the DCE Distributed File Service*. AIXtra On-Line, June 1995.

<http://pscc.dfw.ibm.com/aixtra/issues/may-june/perf.htm>

Ganger, G. R., Patt, Y. N. *Metadata Update Performance in File Systems*. USENIX Symposium on Operating Systems Design and Implementation, November, 1994. pp. 49-60.

Satyanarayanan, M. *A Survey of Distributed File Systems*. Annual Review of Computer Science, 1990, Volume 4, pp. 73-104.

Mummert, L.B., Satyanarayanan, M. *Long Term Distributed File Reference Tracing: Implementation and Experience*. School of Computer Science, Carnegie Mellon University Nov. 1994, CMU-CS-94-213.

JET PROPULSION LABORATORY
NOTIFICATION OF CLEARANCE

05/16/97

TO: J. Bellan
FROM: Logistics and Technical Information Division
SUBJECT: Notification of Clearance - CL 97-0597

The following title has been cleared by the Document Review Services, Section 644, for public release, presentation, and/or printing in the open literature:

The Lewis Number Under Supercritical Conditions

This clearance is issued for the full paper and is valid for U.S. and foreign release.

In the Acknowledgments, cite the Jet Propulsion Laboratory, California Institute of Technology.

Clearance issued by Charlotte Marsh
Charlotte Marsh
Document Review Services
Section 644

(Over)

20620
AUTHORIZATION FOR THE EXTERNAL RELEASE OF INFORMATION

Submit URL (if applicable) or two copies of the abstract or full paper to Document Review, 111-120

CL No. 97-0597

(for DRS use only)

| | | | | |
|--------------------------------|----------------|----------------------|----------------|--------------------|
| Senior JPL Author J. BELLAN | Section 353 | Mail Stop 125/121 | Ext. 4-6959 | Due Date 5/8/97 |
|--------------------------------|----------------|----------------------|----------------|--------------------|

COMPLETE TITLE
The Lewis Number under Supercritical Conditions

☐ Foreign ☐ Domestic Account Code 238-MC717-0-3530 ☐ Premeeting publication
(not to be used for editing)

☐ ABSTRACT (including extended abstract) ☐ Publication on meeting date

☒ FULL PAPER (including viewgraphs, poster, videocassette) ☐ Postmeeting publication

☒ Journal Name International Journal of Heat and Mass Transfer ☐ Poster session

☐ Meeting - Subject _____ ☐ Oral presentation

Sponsoring Society _____

Meeting Date _____ Location _____

☒ BOOK OR BOOK CHAPTER DR 5/12/97

☐ Assigned Laboratory Task OR ☐ Private Venture

☒ PUBLICATION ☐ BROCHURE ☐ NEWSLETTER ☐ For release on the Internet ☐ within JPL
• outside of NASA

URL: _____ FTP: _____

☐ Was previously cleared: Clearance No(s): _____

CL- _____ Date _____ Author(s) _____

CL- _____ Date _____ Author(s) _____

REPORTABLE INFORMATION

THIS WORK: ☐ New technology not previously reported

Nature of this work (please describe) Proposes new length scales for heat and mass transfer at supercritical pressures.

☐ Covers work previously reported in New Technology Report (NTR) No. _____

☐ Provides more information for earlier NTR No(s). _____

FOR TECHNOLOGY REPORTING AND COMMUNICATIONS USE ONLY ☐ Release ☐ Ex Post Facto ☐ Release Delayed or Conditional

Comments: _____

FOR SECTION 644 USE ONLY

Editor _____ Ext. _____ Document No. _____

Customer Code (RTOP No.) _____ Group _____ Condition _____

AUTHORIZATION (please use blue ink)

The signatory in this column attests to the technical accuracy of the subject document.

Justin Bellan 4/30/97
Senior JPL Author Date

W. D. Marshall 5-1-97
Manager/Supervisor or equivalent Date

Print Name and Title of Manager/Supervisor
NOTE: A// full papers and Internet URLs require Section or Project Manager approval.
All abstracts require Group Supervisor approval only.

Technology Reporting and Communications Date
Charlotte Marshall 5/16/97
Document Reviewer Date

Senior JPL Author

J. BELLAN

Section

353

Mail Stop

125/121

Ext.

4-6959

Due

Date

5/8/97

COMPLETE TITLE

of the Lewis Number under Supercritical Conditions

☐ Foreign ☐ Domestic

Account Code 238-MC717-0-3530

(not to be used for editing)

☐ Premeeting publication☐ ABSTRACT (including extended abstract)☐ Publication on meeting day☒ FULL PAPER (including viewgraphs, poster, videocassette)☐ Postmeeting publication☒ Journal Name International Journal of Heat and Mass Transfer☐ Poster session☐ Meeting - Subject☐ Oral presentation

Sponsoring Society

Meeting Date Location

☐ BOOK OR BOOK CHAPTER☐ Assigned Laboratory Task OR☐ Private Venture☐ PUBLICATION ☐ BROCHURE ["newsletter"] ☐ For release on the Internet ☐ within JPL☐ outside of NASA

URL:

FTP:

RECEIVED

Was previously cleared: Clearance No(s):

CL- Date

Author(s) MAY 12 1997

CL- Date

Author(s) JPL TU OFFICE

IMPORTABLE INFORMATION

THIS WORK: ☒ New technology not previously reported

Nature of this work (please describe) Proposes new length scales for heat and mass transfer at supercritical pressures.

☐ Covers work previously reported in New Technology Report (NTR) No.☐ Provides more information for earlier NTR No(s).

OR TECHNOLOGY REPORTING AND COMMUNICATIONS USE ONLY

Comments:

☒ Release ☐ Ex Post Facto ☐ Release Delayed or Conditional

OR SECTION 644 USE ONLY

Editor Ext.

Document No.

Customer Code (RTOP No.)

Group Condition

AUTHORIZATION (please use blue ink)

The signatory in this column attests to the technical accuracy of the subject document.

Senior JPL Author

Date

Manager/Supervisor or equivalent

Date

Technology Reporting and Communications

Date

Print Name and Title of Manager/Supervisor

Document Reviewer

Date

NOTE All full papers and Internet URLs require Section or Project Manager approval. All abstracts require Group Supervisor approval only.

THE LEWIS NUMBER UNDER SUPERCRITICAL CONDITIONS

K. Harstad and J. Bellan
Jet Propulsion Laboratory
California Institute of Technology
pasadena, CA. 91109

Abstract

An effective Lewis number is defined for situations where temperature and **mass fractions** gradients are very large. The definition evolves from a model assuming that derivatives of certain functions are small with respect to those of the dependent variables. In the model, Soret and Dufour effects are included and Shvab-Zeldovich-like variables are defined to remove the coupling between the operators of the differential equations for temperature and mass fractions. Results from calculations using binary systems of compounds, using both isolated fluid drops and interacting fluid drops, show that depending upon the compounds, the effective Lewis number can be 2 to 40 times larger than the traditional Lewis number and that the spatial variation of the two numbers is different. For the values of the thermal diffusion factor used in the calculations, the Soret and Dufour effects are negligible; the discrepancy between the traditional and effective Lewis numbers is entirely due to the difference between the specific enthalpies of the two compounds. Parametric variations show that the effective Lewis number increases with increasing pressure and decreasing surrounding gas temperature. Closer drop proximity in clusters results in sharper peaks in the effective Lewis number due to the increased gradients of the dependent variables.

1. Introduction

The Lewis number is a measure of the importance of heat diffusion to the mass diffusion and therefore provides an indication of what process controls a phenomenon being studied. For example, in gases usually $Le = O(1)$ which means that heat and mass diffusion proceed at similar rates. Departures from unity Le in *gases* have been discussed by Law et al. [1], Haworth and Poinot [2], Lee et al. [3], Joulin [4], Echekki and Freziger [5] and others in the context of curved flames; and by Greenberg and Ronney [6] in the context of flame spread over thin and thick solid fuels. In contrast to gases, in liquids $Le = O(10) - O(100)$ indicating that heat diffusion is faster than mass diffusion.

All existing studies of Le effects in gases have discussed departures from the preferred unity assumption (because it enables an easier mathematical treatment), but none has questioned the validity of the Le definition to portray the relative importance of heat and mass diffusion. This is because the definition of the Lewis number for gases and liquids is straightforward when the molar flux depends only upon the mole fraction gradients and the heat flux depends only upon

the temperature gradient. However, this is not the most general situation, and is certainly not applicable to a general fluid. The present study is devoted to the investigation of departures from the traditional definition of Le for general fluids.

Fluctuation-dissipation theory provides the most general framework for defining the heat and mass diffusion coefficients. Within the formalism of Keizer's fluctuation-dissipation theory [7], [8], the mass diffusivity and thermal diffusivity appear as the diagonal elements of a transport matrix that relates the gradients of the chemical potentials and of the temperature to the molar and heat fluxes as follows:

$$\vec{J}_i = L_{iq} \nabla \beta - \sum_j^N L_{ij} \nabla (\beta \mu_j), \quad \vec{q} = L_{qq} \nabla \beta - \sum_j^N L_{qj} \nabla (\beta \mu_j) \quad (1.1)$$

where L_{ij} are the Fick's diffusion elements, L_{qq} is the Fourier thermal diffusion element, L_{jq} are the Soret diffusion and L_{qj} are the Dufour diffusion elements. The Onsager relations state that $L_{ij} = L_{ji}$ and $L_{iq} = L_{qi}$. From conservation of fluxes and mass in the system one obtains the additional relations $\sum_i^N m_i J_i = \vec{0}$ and $\sum_i^N L_{ij} m_i = 0$ for $j \in [1, N]$ and $j = q$.

Using the thermodynamic relationship

$$d(\beta \mu_j) = \beta (v_j dp - h_j d \ln T) + \left(\sum_i^{N-1} \alpha_{Dji} dX_i \right) / X_j \quad (1.2)$$

where

$$\alpha_{Dij} \equiv \beta X_i \partial \mu_i / \partial X_j = \partial X_i / \partial X_j + X_i \partial \ln \gamma_i / \partial X_j \quad (1.3)$$

one can calculate \vec{J}_i from 1.1 and 1.2. This formalism shows that the classical definition of Le can no longer indicate the relative importance of heat and mass diffusion because of the additional contributions that appear as nondiagonal terms. Thus, there is a need to identify what is the equivalent of Le , called here Le_{eff} , under general conditions and investigate characteristic values of this number. We are particularly interested in the behavior of compounds under supercritical conditions because of the relevance to liquid rocket propulsion, gas turbine engines and Diesel engines.

In this paper we present a formalism for a definition of Le_{eff} and show that under supercritical conditions the existence of the nondiagonal terms in the transport matrix enhances the heat diffusion and decreases the mass diffusion, resulting in Le_{eff} larger than Le by a factor that varies from approximately 2 to 40 depending on the compounds and on the particular conditions of the calculation. Additionally, we show that Le_{eff} is a nonmonotonic function of Le , and thus that the variation of Le cannot be considered to represent even a relative qualitative estimate of the importance of heat and mass diffusion. In Section 2 we develop the expression for Le_{eff} for a binary component fluid in a general one-dimensional geometry; the analysis can be easily extended to a multicomponent fluid in multidimensions. In Section 3 we calculate Le_{eff} for both isolated and collections of spherical entities (fluid drops) of LO_x in fluid H_2 at high pressures and investigate the importance of the thermal diffusion factor upon the results. Results are also presented for isolated C_7H_{16} fluid drops in fluid N_2 to identify the impact of the compounds identity upon the results. Finally, Section 4 is devoted to conclusions.

2. Model

In a one dimensional configuration, the species and energy equations for a binary component fluid can be written as follows:

$$\rho \frac{\partial Y_1}{\partial t} + \rho u \frac{\partial Y_1}{\partial r} = m_1 \nabla \cdot \vec{J}, \quad \rho \frac{\partial Y_2}{\partial t} + \rho u \frac{\partial Y_2}{\partial r} = -m_1 \nabla \cdot \vec{J} \quad (2.1)$$

$$nC_p \left(\frac{\partial T}{\partial t} + u \frac{\partial T}{\partial r} \right) = \alpha_v T \left(\frac{\partial p}{\partial t} + u \frac{\partial p}{\partial r} \right) - \nabla \cdot \vec{q} + \Phi_v - m_1 (h_1/m_1 - h_2/m_2) \nabla \cdot \vec{J} \quad (2.2)$$

where $\alpha_v = [(\partial v / \partial T)_p x_1] / v$, $J = -J_{1r} = (m_2/m_1) J_{2r}$. As shown by Eqs.1.1, the general form of J and $q = -q_r$ are

$$\begin{aligned} J &= A_J \frac{\partial Y_1}{\partial r} + B_J \frac{\partial T}{\partial r} + C_J \frac{\partial p}{\partial r} \\ q &= A_q \frac{\partial T}{\partial r} + C_q \frac{\partial Y_1}{\partial r} + B_q \frac{\partial p}{\partial r} \end{aligned} \quad (2.3)$$

Expressions of the gradients multiplicative coefficients in Eq. 2.3 appear in the Appendix.

The terms proportional to the gradients of the dynamic pressure in the expressions for J and q will be neglected in the following because those gradients are proportional to Ma^2 and $Ma \ll 1$, while coefficients C_J and B_q are of same magnitude as other coefficients in the equations; spatial variations of p' were confirmed to be small by results from calculations of isolated entities of LO_x in fluid H_2 at high pressures [10]. The viscous dissipation term has been neglected as well because it is expected to be much smaller than the other terms in Eq. 2.2.

If the set $\Gamma = (Y, T)$ is considered a vector primitive variable, the differential operator $\mathcal{L}\Gamma = \rho \partial \Gamma / \partial t + \rho u \partial \Gamma / \partial r - (1/r^s) \partial (r^s \mathcal{D} \partial \Gamma / \partial r) / \partial r$, where $s = 0$ for planar geometry and $s = 2$ for spherical geometry, represents the set of conservation equations $\mathcal{L}\Gamma = 0$, where \mathcal{D} is a generic diffusion coefficient matrix. When Fick's and Fourier's laws accurately describe molar and heat fluxes respectively, the operators for the two variables Y_1 and T are uncoupled because the diffusion term in the equation for each variable contains only derivatives of that variable; \mathcal{D} is diagonal. In this situation, one defines the traditional Le as the ratio of the diffusive length scales of the temperature and mass fractions; this ratio is calculated using the coefficients of the diffusive terms. In the more general situation where the flux matrix is given by Eq.2.3 instead of the Fick and Fourier laws, the differential operators for the two variables are no longer uncoupled because in each equation the diffusion term contains derivatives of **both** variables. The differential operators are now coupled, and this coupling prohibits a simple definition of appropriate diffusion length scales for heat and mass transfer.

Similar to the classical situation where Le relates the diffusive length scales of the mass fractions and temperature given by the coefficients of the diffusive terms when the differential operators of the species and temperature equations are uncoupled, and thus the diffusion term in the differential operator is given by multiplying a diagonal matrix with the spatial derivative, one must find here equivalent variables for which the matrix of the system of equations 2.1 and 2.2 has a diagonal form. Given the complexity of Eqs. 2.1, 2.2 and 2.3, a simple, accurate combination of variables cannot be found *a priori*. Therefore, the strategy is here to find a solution that will be valid under certain assumptions.

The first assumption is that of a boundary layer spatial variation at a location that would be a surface under subcritical conditions, $r = R_d$, in which case the medium for $r < R_d$ is a liquid

(component 1) and the medium for $r > R_d$ is a gas (component, 2). The analysis will be then valid for $|R_d - r| \ll R_d$. In subcritical conditions, the liquid evaporates (except for the particular case of saturation) and thus $pu = F_{ems}$; under supercritical conditions one may still define the flux in the same manner although its meaning is no longer that of evaporation. The second assumption is that of quasi-steady behavior; although under supercritical conditions a quasi-steady behavior is not necessarily attained (because the value of the density ratio $\rho(R_d^+)/\rho(R_d^-)$ does not remain $\ll 1$ during the calculation), this assumption is appropriate for finding order of magnitude scales rather than an entirely accurate solution for the variables. It is the form of the steady, convection-diffusion equation solution that provides the intuition about the assumptions to be further made in the model. This form is an exponential dependence on a spatial integral multiplied by a more weakly varying function [9].

The point of departure for finding an approximate solution are Shvab-Zeldovich-like variables [11] that are combinations of Y_1 and T . In the Shvab-Zeldovich formalism for transient combustion in a diffusive-convective system, linear combinations of variables are used in conjunction with a series of assumptions to eliminate the reaction term from all but one equation and render the conservation equations easier to solve. In the present context, the combined variables

$$\Omega_Y \equiv Y_1 - \omega_T T \text{ and } \Omega_T \equiv T - W_Y Y_1 \quad (2.4)$$

are defined to diagonalize the operators of the differential equations; the quantities ω_T and ω_Y are calculated below by satisfying the conservation equations. Once Eqs. 2.4 are replaced into the original equations 2.1, 2.2 and 2.3, Ω_Y and Ω_T can be shown to be approximately governed by the following equations for appropriately chosen ω_T and ω_Y

$$\rho \frac{\partial \Omega_Y}{\partial t} + F_{ems} \frac{\partial \Omega_Y}{\partial r} = \frac{1}{r^s} \frac{\partial}{\partial r} (r^s \rho D_{eff} \frac{\partial \Omega_Y}{\partial r}) \quad (2.5)$$

$$\rho \frac{\partial \Omega_T}{\partial t} + F_{ems} \frac{\partial \Omega_T}{\partial r} = \frac{1}{r^s} \frac{\partial}{\partial r} [r^s (m \lambda_{eff} / C_p) \frac{\partial \Omega_T}{\partial r}] \quad (2.6)$$

Equations 2.5 and 2.6 are obtained under the assumption that spatial and temporal derivatives of functions ω_T and ω_Y are smaller than those of Ω_Y and Ω_T and can thus be neglected. This assumption is satisfied if Eqs. 2.5 and 2.6 are quasi-steady and if the multipliers of the exponential functions which are the characteristic solutions of the diffusion-convection equation have a smaller variation than the exponential functions. Quasi-steadiness of Eqs. 2.5 and 2.6 is satisfied if $(F_{ems})^2 \gg \rho^2 D_{eff} \partial / \partial t$ and $(F_{ems})^2 \gg (m \rho \lambda_{eff} / C_p) \partial / \partial t$. Small variation of the multipliers with respect to the exponential functions occurs if $F_{ems} \Delta r > \rho D_{eff}$ and $F_{ems} \Delta r > m \lambda_{eff} / C_p$, where Δr is the grid size.

The effective transport coefficients in Eqs. 2.5 and 2.6 are calculated from the original equations as follows:

$$\rho D_{eff} = m_1 A_J - \omega_T m C_q' / C_p \quad (2.7)$$

$$\lambda_{eff} = A_q' - \omega_Y (m_1 / m) C_p B_J \quad (2.8)$$

where

$$A'_q \equiv A_q - m_1(h_1/m_1 - h_2/m_2)B_J \text{ and } C'_q \equiv C_q - m_1(h_1/m_1 - h_2/m_2)A_J \quad (2.9)$$

and

$$\omega_T = \sigma m_1 C_p B_J / m \text{ and } \omega_Y = -\sigma C'_q \quad (2.10)$$

where σ is the positive root of the second order algebraic equation

$$(m_1/m)C_p B_J C'_q \sigma^2 + [A'_q - (m_1/m)C_p A_J] \sigma - 1 = 0 \quad (2.11)$$

the other root being unphysical as it leads to singular behavior. These equations allow the calculation of D_{eff} , λ_{eff} and $Le_{eff} \equiv \lambda_{eff} / (n C_p D_{eff})$ once the values of the dependent variables are known.

Although the above analysis is strictly valid only within a boundary layer, it is also conceptually correct in any region where there are large variations of the dependent variables. Thus, the above expressions show the correct transport scales for any region of steep gradients. As such, the ratio of the effective transport coefficients will be calculated below and compared to that of the conventional transport coefficients for specific situations involving large dependent variables gradients.

To illustrate the model, calculations are performed for spherical fluid drops, either isolated or in clusters where they may collectively interact. The general model for isolated fluid drops is described in [10] and is based upon the fluctuation-dissipation theory discussed above whose main results are Eqs. 2.1, 2.2 and 2.3. Additional to the conservation equations 2.1 and 2.2, the model of Harstad and Bellan [10] also solves a mass conservation equation. The boundary conditions at the evolving interface initially between pure LO_x and mainly H_2 fluid, and in the far field are also described in detail in [10]. The calculation of the equations of state is described elsewhere [14] and the models for the transport coefficients is discussed in Harstad and Bellan [10]. For cluster studies, there are additional mass, species and energy conservation equations relating the behavior of all entities in the cluster [12], and boundary conditions between the cluster and its surroundings.

3. Results

To illustrate the difference between the traditional Le and Le_{eff} we present calculations obtained from the solution of isolated fluid drops and clusters of fluid drops of LO_x in H_2 at supercritical conditions. In order to evaluate the importance of the Soret and Dufour terms, we also present results from isolated fluid drop calculations with null α_T as well as with one non null value smaller than the baseline choice of $\alpha_T = 0.05$ [13]. Finally, to investigate possible departures from the conclusions based on results from the $LO_x - H_2$ system, we also present results for isolated C_7H_{16} fluid drops in fluid N_2 ; obviously, a myriad of binary systems can be investigated and by its nature the present study cannot be exhaustive.

3.1. Isolated fluid drops: the $LO_x - H_2$ system

3.1.1. Baseline behavior

Figure 1 illustrates the radial variation of Le and Le_{eff} at different times for an isolated fluid drop having $R_d^0 = 50 \times 10^{-4}$ cm and $T_{d,b}^0 = 100$ K (the fluid drop temperature is assumed initially

uniform), in far field surroundings characterized by $T_{si}^0 = 1000$ K, $p = 80$ MPa and $Y_{si}^0 = O$. The fluid drop is initially composed of pure LO_x ($T_c = 154.6$ K, $p_c = 5.043$ MPa), while the surrounding is hydrogen ($T_c = 33.2$ K, $p_c = 1.313$ MPa); in order to avoid an initial unphysical discontinuity, a small amount of oxygen exists initially in the drop surroundings, its distribution vanishing with increasing r . The far field conditions $T_e = 1000$ K and $Y_{1e} = O$ are at a distance $(R_{si}^0 - R_d^0)$ from the drop interface, where $R_{si}^0 = 0.1$ cm.

The spatial variation of Le_{eff} is essentially different of that of Le in that it is nonmonotonic even after the memory of the initial condition is lost. This is because Le_{eff} implicitly but completely accounts for Y_1 and T gradients effects; these Y_1 and T gradients do not occur at the same location under supercritical conditions. Thus, the spatial variation of Le_{eff} is directly related to the variation of Y_1 and T gradients as follows: For small r , the shallow part of the curves corresponds mostly to the large $\partial T / \partial r$, Y_1 being mostly uniform, and the temporal increase of Le_{eff} is due to the increased T . The strongly increasing branch of Le_{eff} corresponds to the region of large $\partial Y_1 / \partial r$ and the location of the maximum Le_{eff} is directly related to the maximum Y_1 gradient. Finally, the decreasing part of the Le_{eff} curves corresponds to the decreasing $\partial Y_1 / \partial r$ and the asymptotic leveling of T . In contrast, the Le spatial variation reflects only the dependence of D_T and D_m upon composition and T . An elimination of the spatial variation between Le and Le_{eff} results in the plots presented in Fig. 2: Le_{eff} versus Le at different times. Examination of the curves in Figs. 1 and 2 indicates that the additional coupling terms result in an enhancement of the thermal diffusivity with respect, to the mass diffusivity. More precisely, tedious manipulations of Eqs. 2.7-2.11 and 5.1-5.6 in the Appendix show that in fact the thermal diffusivity is effectively increased whereas the mass diffusivity is effectively decreased. For the conditions used to obtain the results depicted in Fig. 1, the ratio Le_{eff}/Le is approximately 20 in the inner part of the interface, whereas on the outer side of the interface it reaches a maximum of 60 and a minimum of 3.

The fact that Le is a multivalued function of Le_{eff} (see Fig.2) is a warning that Le cannot be even considered a qualitative estimate of the true relative importance of heat to mass diffusion at different spatial locations. Moreover, whereas the values of Le_{eff} indicate that heat diffusion exceeds mass diffusion at all locations, Le indicates erroneously that mass diffusion dominates heat diffusion at all times for $r \leq R_d^0$. The almost-complete coincidence of all curves in Fig. 2 indicates that for a given geometry and initial conditions, at each spatial position there is an almost-unique relationship between the ratio of the transport coefficients and the ratio of the effective transport coefficients (but not vice versa). Since both the transport coefficients and the effective transport coefficients depend upon Y_1 and T (whose variation is governed by the conservation equations) this coincidence is not obvious and its meaning is not immediately apparent. Further results presented below for the $C_7H_{16} - N_2$ system indicate that the self-similarity is not a property of the conservation equations and is instead related to the system of compounds.

3.1.2. Parametric variation

Plots of Le and Le_{eff} at $t = 2 \times 10^2$ s for same initial conditions as the baseline calculations except for p , appear in Fig. 3. Increasing p decreases both D_m and D_T (see Fig.4), however, $D_T \equiv \lambda / (nC_p)$ is a stronger function of p . The spatial variation of all transport properties results from the different p in the far field, and from the combined effect of the different, p upon the composition, ρ and T in the near field of the initial drop boundary [10]. In the inner region of mild gradients, both Le and Le_{eff} show similar variations, however, the absolute values differ by

a factor of approximately 20. In the far field region (which similarly to the inner region has small gradients), both Le and Le_{eff} show an asymptotic behavior, their values differing by a factor of approximately 3. The large difference of variation (approximately a factor of 50) occurs in the region of strong gradients in accord with the boundary layer analysis. The narrowing of the width between the increasing and the decreasing branches of Le_{eff} indicates the reduction in scales with increasing p . The variation of Le_{eff} with Le depicted in Fig. 3 indicates that in the low and high Le regime there is an almost unique relationship to Le_{eff} independent of p , whereas the influence of p is mainly felt in the intermediate Le regime which occurs in the region of large gradients.

Far field temperature effects upon the variation of Le and Le_{eff} are illustrated in Fig. 5 at $t = 2 \times 10^{-2}$ s for two temperatures at three values of p . In the lower p range, the T and Y_1 gradients occur at increasing distance with increasing temperature, whereas in the higher p regime the distance between the largest gradients of T and Y_1 becomes less sensitive to temperature. Unlike the variation of Le_{eff} with Le as a function of p , the relationship between Le and Le_{eff} is sensitive to T_{si}^0 over the entire range of Le .

The variation of Le and Le_{eff} with the initial fluid drop size is depicted in Fig. 6 and shows the increase in scales with increasing initial size.

To investigate the importance of Soret and Dufour effects on the above results, calculations were performed with $\alpha_T = 0$ and 0.01 to compare with the baseline calculations where $\alpha_T = 0.05$. The results from the three sets of calculations were virtually indistinguishable indicating that for the range of α_T explored, the Soret and Dufour terms are negligible. This result is in apparent contradiction with the difference in magnitude and variation of Le and Le_{eff} . However, careful examination of Eqs. 2.3 and 5.2 in the Appendix shows that the contribution to the molar flux from the temperature gradient contains two terms: the first is the difference in the ratios of the molar enthalpies divided by the molar masses, and the second is the Soret term. Spatial plots of the molar enthalpy (not presented) show that the LO_x molar enthalpy is smaller than that of H_2 . Since additionally the molar mass of oxygen is one order of magnitude larger than that of hydrogen, this renders the first term in Eq. 5.2 in the Appendix very large compared to the Soret term. The present conclusions depend on the uncertain value range for α_T ; to our knowledge, there is no data providing α_T for the $LO_x - H_2$ system as a function of T , p and Y_1 .

3.2. Clusters of fluid drops: the $LO_x - H_2$ system

To investigate the effect of fluid drops proximity on the relative importance of both conventional and effective heat and mass diffusion, calculations were performed with spherical clusters of these drops. The detailed model for the fluid drops interactions is described elsewhere [12]; the only results discussed here are those pertinent to Le and Le_{eff} .

Due to the essentially diffusive behavior at supercritical conditions, interactions among fluid drops are not expected unless these are in close proximity. The proximity of the fluid drops is measured by a 'sphere of influence' around each drop. This sphere of influence is centered at the drop center and has a radius, R_{si} , which is half of the distance between adjacent drops. Transfer from the cluster surroundings to the cluster is modeled using the Nusselt number concept, [12]. As an example, in the baseline calculation with $R_d^0 = 50 \times 10^{-4}$ cm, $R_{si}^0 = 2R_d^0$, $R_C^0 = 2$ cm, $T_{d,b}^0 = 100$ K (T_d^0 is uniform inside the drop), $T_{si}^0 = T_e = 1000$ K, $p_e = 80$ MPa and $Y_{1e} = 0$, the number of drops in the cluster is 5.92×10^6 .

Results illustrating the difference in variation for both Le and Le_{eff} with increasing R_{si}^0/R_d^0 for

two different pressures are depicted in Fig. 7. Decreasing R_{si}^0/R_d^0 results in an increase in Le and the effect is more pronounced at larger pressures, however the maximum value attained is always at the edge of the sphere of influence and remains constant with pressure and drop packing. In contrast, Le_{eff} attains its maximum inside the sphere of influence, at the location of maximum Y_1 gradients [12] as already explained above. Additionally, while the maximum Le_{eff} value remains constant, with drop packing, it increases substantially with pressure in agreement with the known larger augmentation of heat diffusion with respect to mass diffusion as the pressure increases. Examination of Fig. 7b shows that a factor of 4 increase in pressure induces approximately a 25% increase in the maximum value of Le_{eff} .

Since gradients at the edge of the cluster boundary are influenced by Nu_t , the value of Nu_C was varied from 10^2 (baseline) to 10^5 in increments of factors of 10. The plots appearing in Fig. 8 show the relative insensitivity of the results to Nu_c : it is only the size of the cluster that slightly increases (due to increased heat transfer) when Nu_c changes by three orders of magnitude, but the maximum value of either Le or Le_{eff} is not affected. However, the increase in Nu_c corresponds to a reduction in T at a given location as the volume of the sphere of influence is increased; this affects the transport properties and induces a reduction in Le . In contrast, no such monotonic behavior is observed for Le_{eff} due to the combined effect of the transport properties variation and the reduction in the gradients at larger Nu_c .

3.3. Isolated fluid drops: the $C_7H_{16} - N_2$ system

The validity of the above conclusions for other systems has been investigated by performing calculations for an application relevant to gas turbine engines and Diesel engines: the $C_7H_{16} - N_2$ system. Examination of the molar enthalpies of the two compounds shows that of n-heptane to be smaller than that of nitrogen; since the molar mass of n-heptane is larger than that of nitrogen, Soret and Dufour effects are again expected to be negligible. To ascertain this expectation, calculations were performed with $\alpha_T = 0.0, 0.01$ and 0.05 and it was found that the results were virtually indistinguishable.

Figure 9 illustrates results from calculations for isolated heptane drops in nitrogen for the following conditions: $R_d^0 = 50 \times 10^{-4}$ cm, $R_{si}^0 = 0.03$ cm, $T_{d,b}^0 = 400$ K (T_d^0 is uniform inside the drop), $T_{si}^0 = T_e = 1000$ K, $p_e = 20$ MPa and $Y_{1e} = O$. The ratio of Le_{eff} to Le is only approximately 2 for the maximum value independent of location, and approximately 3 locally. Similar to the $LO_x - H_2$ system, the variations of Le_{eff} and Le with r are different indicating again that Le is not a good qualitative measure of relative heat to mass transfer. Plots of Le_{eff} versus Le (not illustrated) paralleling those of Fig. 2 do not show the self-similar variation which seems to be a peculiarity of the $LO_x - H_2$ system.

4. Summary and conclusions

A model has been developed to define an effective Lewis number for situations where large gradients of species and temperature exist in a system. The model is based upon the assumption that derivatives of certain functions are small with respect to those of the dependent variables. Shvab-Zeldovich-like variables are defined to eliminate the coupling of the operators of the differential equations for species and energy. Based upon the new equations for the Shvab-Zeldovich-like

variables, an effective diffusivity and thermal conductivity are defined and further calculated incorporating Soret and Dufour effects.

Results obtained for the isolated LO_x fluid drop in H_2 show that the effective Lewis number can be larger than the Lewis number by a factor of 40. Additionally, the traditional Lewis number and effective Lewis number have different, spatial variations indicating that the traditional Lewis number is not even a qualitative measure of the relative importance of heat and mass transfer. Calculations performed by varying the value of the thermal diffusion factor indicate that it is not the Soret and Dufour terms that are responsible for the difference between the traditional and effective Lewis numbers. Instead, it is found that the difference between the specific enthalpies of the two compounds is responsible for the enhancement in heat diffusion over mass diffusion. Similar calculations performed for fluid n-heptane drops in nitrogen showed the same trends in that the Soret and Dufour terms were unimportant within the range of values used for the thermal diffusion factors. For the n-heptane - nitrogen system, the effective Lewis number was only a factor of 2 to 3 larger than the traditional Lewis number. The uncertainty in the value and variation of the thermal diffusion factor with temperature, pressure and species molar fraction does not allow a definitive conclusion as to the importance of Soret and Dufour terms.

Parametric studies show that the effective Lewis number increases with increasing pressure and decreasing temperature, and that closer drop proximity results in sharper peaks in the effective Lewis number due to the increased gradients of the dependent variables.

ACKNOWLEDGMENT

This research was conducted at the Jet Propulsion Laboratory under sponsorship from the National Aeronautics and Space Administration, the George C. Marshall Space Flight Center with Mr. Klaus W. Gross as technical contract monitor and from the National Aeronautics and Space Administration, the Lewis Research Center with Drs. Edward Mularz and Daniel L. Bulzan as technical contract monitors. Their continuing interest and support are greatly appreciated.

5. APPENDIX

The expressions for the elements of the flux matrix are as follows:

$$A_J = (m/m_1)nD_m\alpha_D \quad (5.1)$$

$$B_J = (m_2/m)nD_m\{(m_1m_2X_1X_2/m)(h_2/m_2 - h_1/m_1)/(R_uT^2) + X_1X_2\alpha_T/T\} \quad (5.2)$$

$$C_J = (m_2/m)nD_m(m_1m_2X_1X_2/m)(v_1/m_1 - v_2/m_2)/(R_uT) \quad (5.3)$$

$$A_q = \lambda + (\alpha_T R_u T)nD_m(m_1m_2X_1X_2/m)(h_2/m_2 - h_1/m_1)/(R_uT^2) \quad (5.4)$$

$$C_q = [m^2/(m_1m_2)]nD_m\alpha_D\alpha_T R_u T \quad (5.5)$$

$$B_q = nD_m\alpha_T(m_1m_2X_1X_2/m)(v_1/m_1 - v_2/m_2) \quad (5.6)$$

According to the Gibbs-Duhem relationship $\alpha_D = \alpha_{D1} = \alpha_{D2}$ where $\alpha_{Di} = 1 + X_i(\partial \ln \gamma_i / \partial X_i)_{T,p}$.

References

- [1] Law, C. K., Sung, C. J. and Sun, C. J., On the aerodynamics of flame surfaces, to appear in Annual Review of Heat Transfer, Vol. VIII, Ed. C. L. Tien
- [2] Haworth, D. C. and Poinso, T. J., Numerical simulations of Lewis number effects on turbulent premixed flames, *J. Fluid Mech.*, 244, 405-436 (1992)
- [3] Lee, J. G., Lee, T. W., Nye, D. A. and Santavice, D. A., Lewis number effects on premixed flames interacting with turbulent Karman vortex streets, *Combust. Flame*, 100(1-2), 161-168 (1995)
- [4] Joulin, G., On the response of premixed flames to time-dependent stretch and curvature, *Combust. Sci. and Tech.*, 97(1-3), 219-229 (1994)
- [5] Echekki, T. and Ferziger, J. H., Studies of curvature effects on laminar premixed flames - Stationary cylindrical flames, *Combust. Sci. and Tech.*, 90(1-4), 231-252 (1993)
- [6] Greenberg, J. B. and Rormey, P. D., Analysis of Lewis number effects in flame spread, *Int. J. Heat Mass Transfer*, 36(2), 315-323 (1993)
- [7] Keizer, J., *Statistical Thermodynamics of Nonequilibrium Processes*, Springer-Verlag, New York, 1987
- [8] Peacock-Lopez, E. and Woodhouse, L., Generalized transport theory and its application to binary mixtures, In *Fluctuation Theory of Mixtures*, Advances in Thermodynamics, Vol. 2, Eds. Matteoli, E. and Mansoori, G. A., Taylor and Francis, 301-333, 1983
- [9] Bellan, J and Cuffel, R., A theory of non-dilute spray evaporation based upon multiple drop interaction, *Combust. and Flame*, 51(1), 55-67 (1983)
- [10] Harstad, K and Bellan, J., "Isolated fluid oxygen drop behavior in fluid hydrogen at rocket chamber pressures", submitted (1997)
- [11] Williams, F. A., *Combustion Theory*, Addison-Wesley (1965)
- [12] Harstad, K and Bellan, J., Interactions of fluid oxygen drops in fluid hydrogen at rocket chamber pressures, submitted (1997)
- [13] Bird, R. B., Stewart, W. E. and Lightfoot, E. N., *Transport Phenomena*, John Wiley and Sons, 1960
- [14] Harstad, H. G. , Miller, R. S., and Bellan, J., Efficient high pressure state equations, accepted for publication, *A. I. Ch.* 11., 1997

NOMENCLATURE

| | |
|-----------|------------------------------------|
| C_p | heat capacity at constant pressure |
| D | diffusion coefficient |
| F_{ems} | emission flux |
| h | molar enthalpy |
| J | molar flux |
| L | elements of the transport matrix |
| Le | Lewis number |
| m | molar mass |
| Ma | Mach number |
| n | number of moles per unit volume |
| N | number of species |
| Nu_c | Nusselt number |
| p | pressure |
| q | heat flux |
| r | generic coordinate |
| R_d | fluid entity radius |
| R_u | universal gas constant, |
| t | time |
| T | temperature |
| u | velocity |
| v | molar volume |
| X | mole fraction |
| Y | mass fraction |

GREEK

| | |
|------------|--------------------------|
| α_D | mass diffusion factors |
| α_T | thermal diffusion factor |
| α_v | thermal expansion ratio |
| β | $1/(RVT)$ |
| γ | activity coefficient |
| Δr | grid size |
| η | viscosity |
| λ | thermal conductivity |
| μ | chemical potential |
| ρ' | density |
| τ | stress tensor |
| Φ_v | viscous dissipation |

SUBSCRIPTS

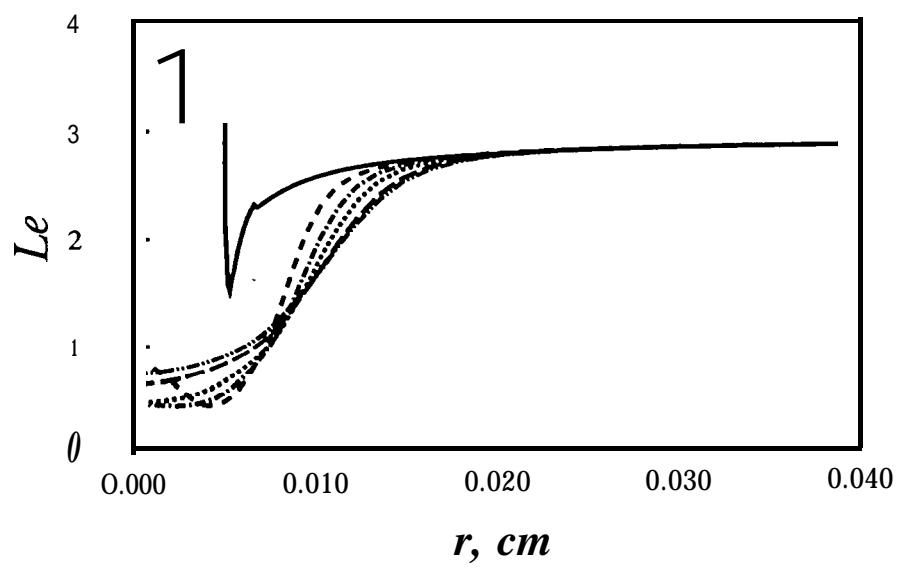
| | |
|--------|--|
| b | fluid entity interface, at $r = R_d$ |
| c | critical point property |
| C | cluster |
| d | fluid drop |
| e | external |
| eff | effective |
| i, j | species |
| m | mass |
| si | at the edge of the sphere of influence |
| T | thermal |

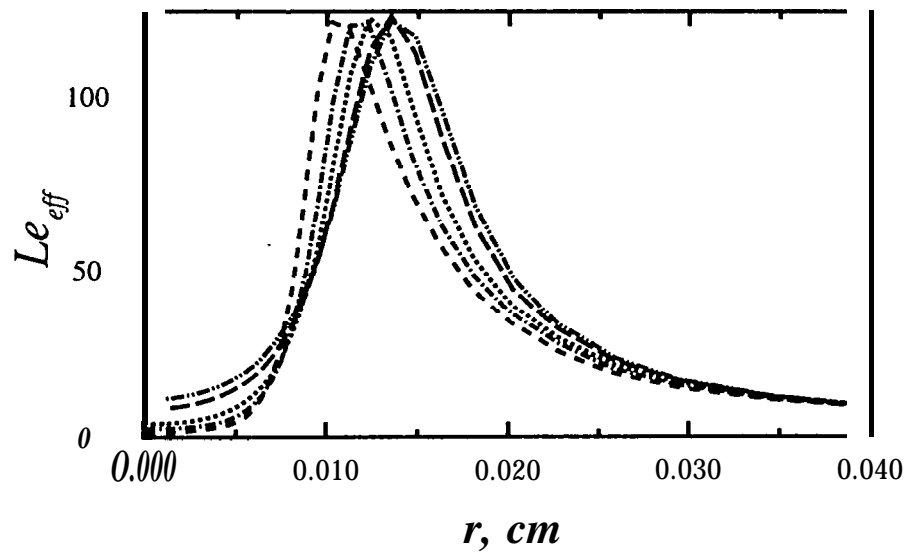
SUPERSCRIPTS

| | |
|---------|---|
| i, j | species |
| o | initial value |
| $+ (-)$ | on the pure $LO_x(H_2)$ side of $r = R_d$ |

FIGURE CAPTIONS

- Fig. 1 Spatial variation of the traditional (a) and effective (b) Lewis numbers at various times for $R_d^0 = 50 \times 10^{-4}$ cm, $R_{si} = 0.1$ cm, $T_{d,b}^0 = 100$ K, $T_{si}^0 = 1000$ K, $Y_{si}^0 = 0$, and $p = 80$ MPa. The curves correspond to the following times: 0.0 s (—), 6×10^{-3} s (- - -), 1.0×10^{-2} s (- . - . -), 1.4×10^{-2} s (· · ·), 2.0×10^{-2} s (— ---), 2.31×10^{-2} S (- . . -).
- Fig. 2 Variation of the effective Lewis number with the traditional Lewis number for the conditions listed in the caption of Fig. 1. The curves are labelled identically to those of Fig. 1.
- Fig. 3 Spatial variation at 2×10^{-2} s of the traditional (a) and effective (b) Lewis numbers and the variation of the effective Lewis number with the traditional Lewis number (c) for several pressures: 10 MPa (- - -), 20 MPa (- . - . -), 25 MPa (· · ·), 40 MPa (— ---), 80 MPa (- . . -). Other initial conditions are those in Fig. 1 caption.
- Fig. 4 Spatial variation of the mass (a) and thermal (b) diffusivities at 2×10^{-2} s for the conditions listed in the caption of Fig. 3; the curves are also labelled identically.
- Fig. 5 Spatial variation at 2×10^{-2} s of the traditional (a) and the effective (b) Lewis numbers, and variation of the effective Lewis number with the traditional Lewis number (c) at 2×10^{-2} s. Plots are for two temperatures and three pressures; the other conditions are those listed in Fig. 1 caption. Curves are labelled as follows: $T_{si}^0 = 1000$ K (—), (- - -) and (- . - . -); and $T_{si}^0 = 500$ K (· · ·), (— ---) and (- - -). Corresponding pressures are: 20 MPa (—) and (· · ·); 40 MPa (- - -) and (- - -); and 80 MPa (- . - . -) and (- . . -).
- Fig. 6 Spatial variation at 2×10^{-2} s of the traditional (a) and the effective (b) Lewis numbers at 25 MPa for initial fluid drop radii 25×10^{-4} cm (- . - . -), 50×10^{-4} cm (—) and 300×10^{-4} cm (· · ·). The other conditions are those of Fig. 1.
- Fig. 7 Spatial variation at 10^{-2} s of the traditional (a) and the effective (b) Lewis numbers for clusters of drops having $R_d^0 = 50 \times 10^{-4}$ cm, $Nu_c = 10^2$, $R_C^0 = 2$ cm, $T_{d,b}^0 = 100$ K, $T_{si}^0 = T_e = 1000$ K and $Y_{si}^0 = Y_e = 0$. Curves are labelled as follows: $R_{si}^0/R_d^0 = 10$ (-----) and (- - -); 5 (— ---) and (- . . -); 2 (- . - . -) and (· · ·). Two pressures are considered: 20 MPa (-----), (- - -) and (- . - . -); and 80 MPa (- - -), (- . . -) and (· · ·).
- Fig. 8 Spatial variation at 10^{-2} s of the traditional (a) and the effective (b) Lewis numbers for $Nu_C = 10^2$ (—), 10^3 (- - -), 10^4 (- . - . -), and 10^5 (· · ·). The other conditions are those of Fig. 7.
- Fig. 9 Spatial variation of the traditional (a) and the effective (b) Lewis numbers for the n-heptane - nitrogen system for several times: 0.0 s (—), 10^{-2} s (- - -), 2×10^{-2} s (- . - . -), 2.25×10^{-2} s (· · ·), 2.5×10^{-2} s (-----), 3.3×10^{-2} s (- . - . -). Other initial conditions are: $R_d^0 = 50 \times 10^{-4}$ cm, $R_{si}^0 = 0.03$ cm, $T_{d,b}^0 = 400$ K, $T_{si}^0 = T_e = 1000$ K, $Y_{1e} = 0$ and $p = 20$ MPa.





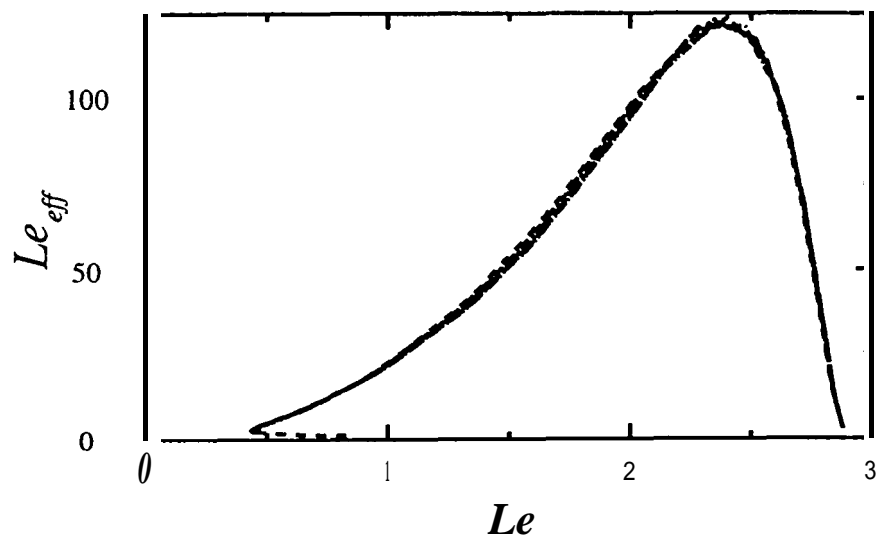


fig 2

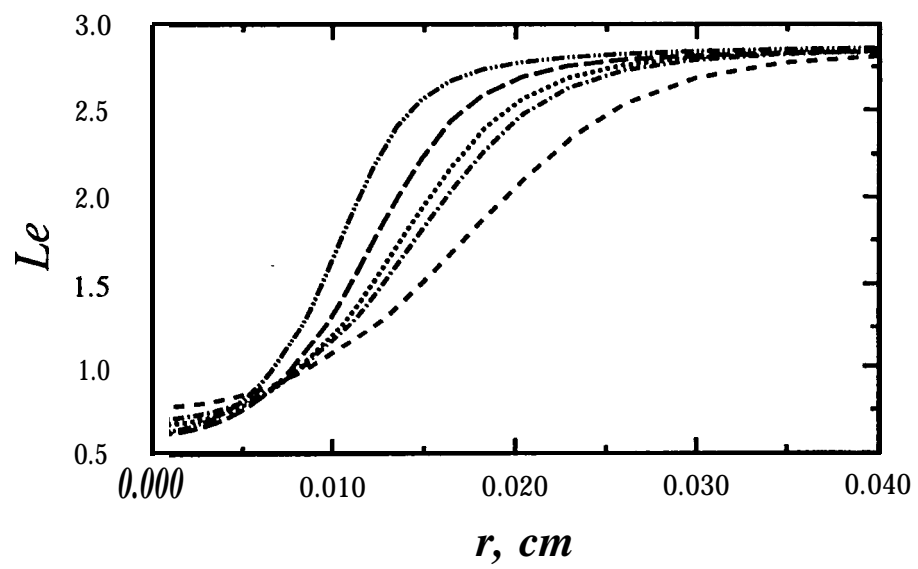
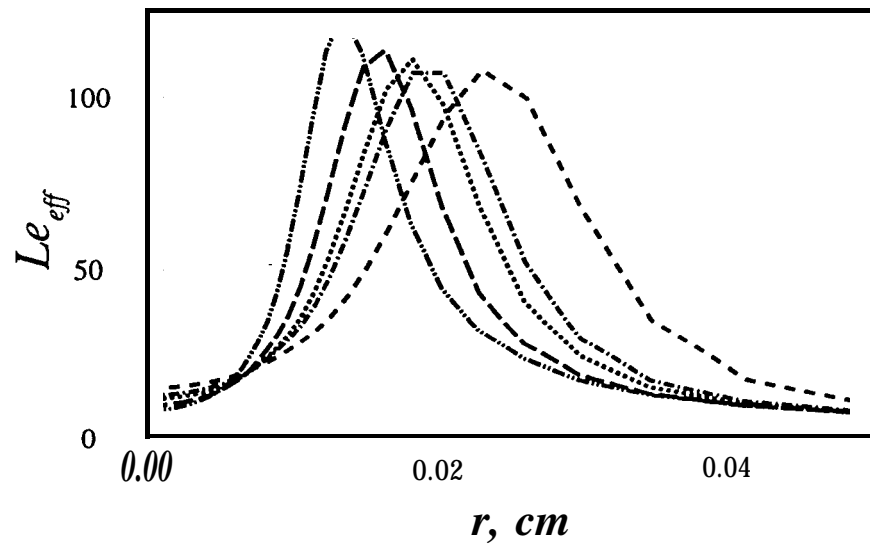
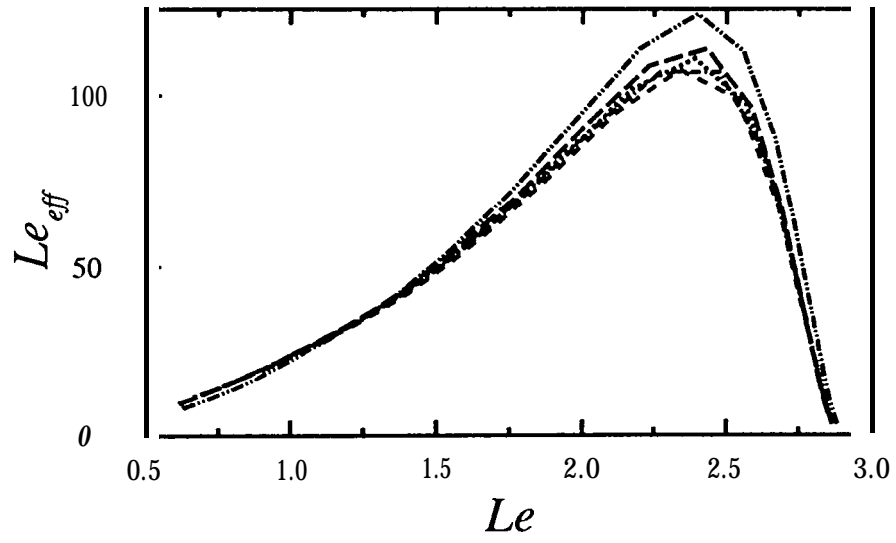


Fig 3a





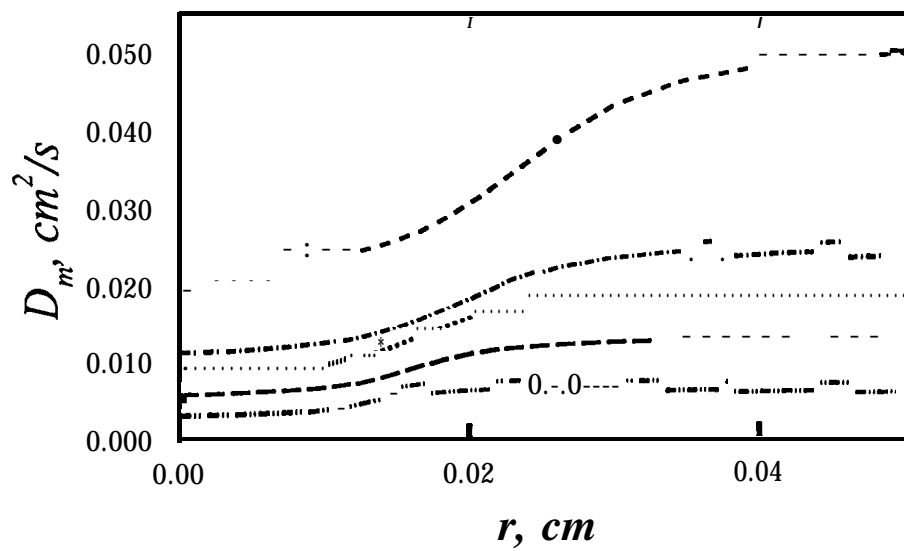


Fig 4a

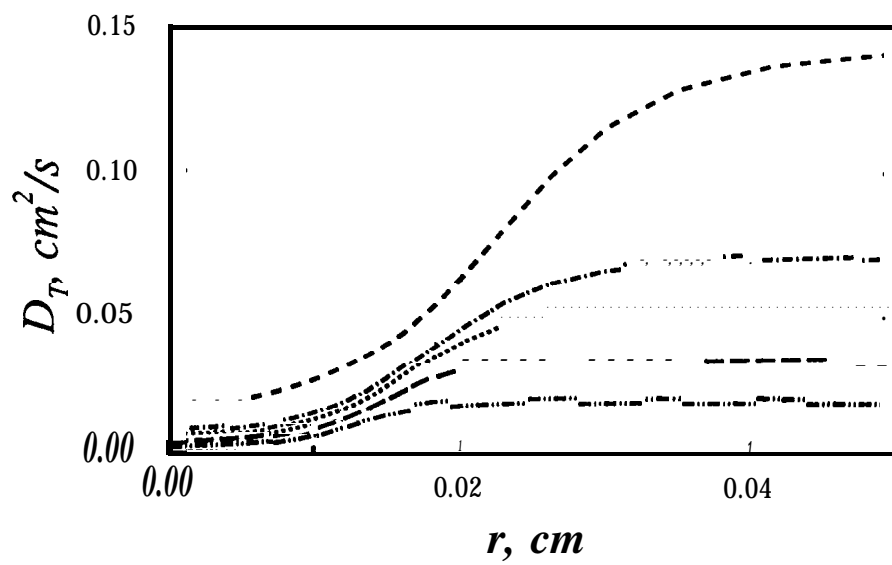


Fig 46

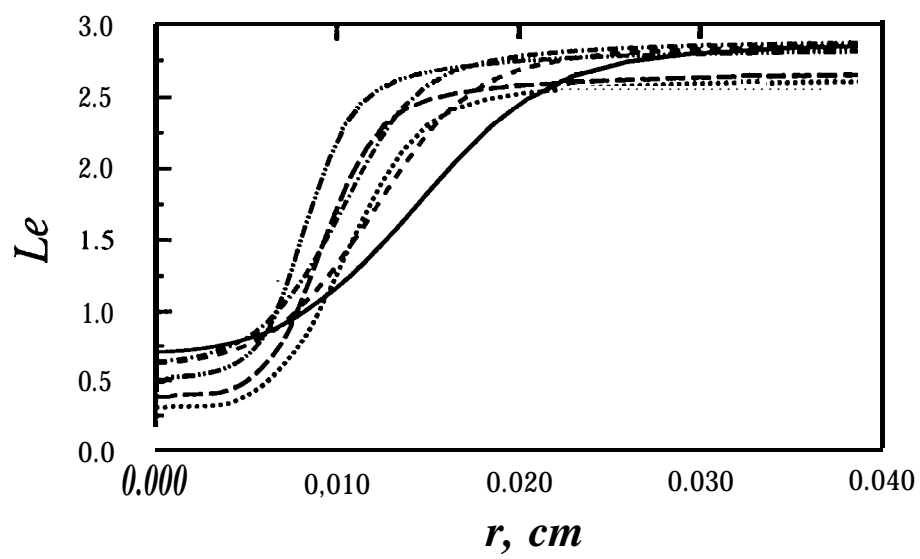
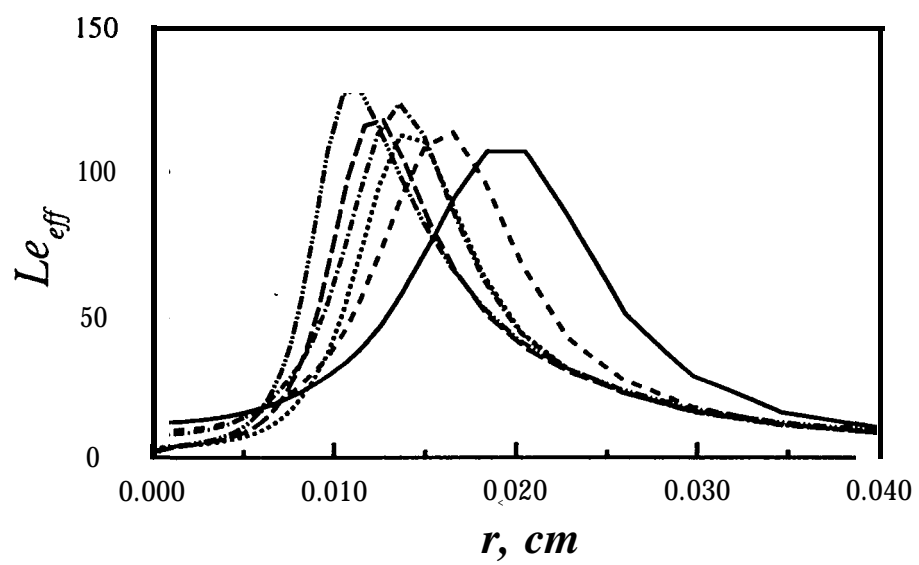
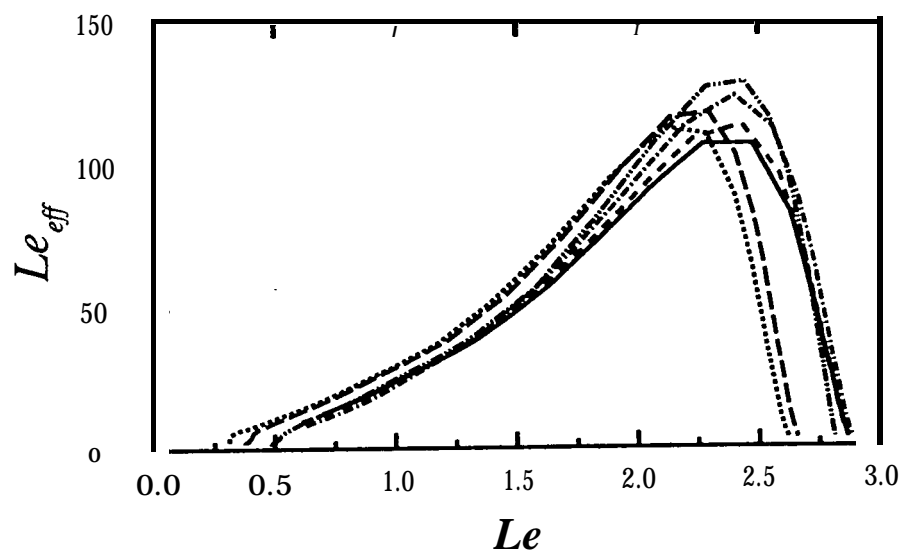
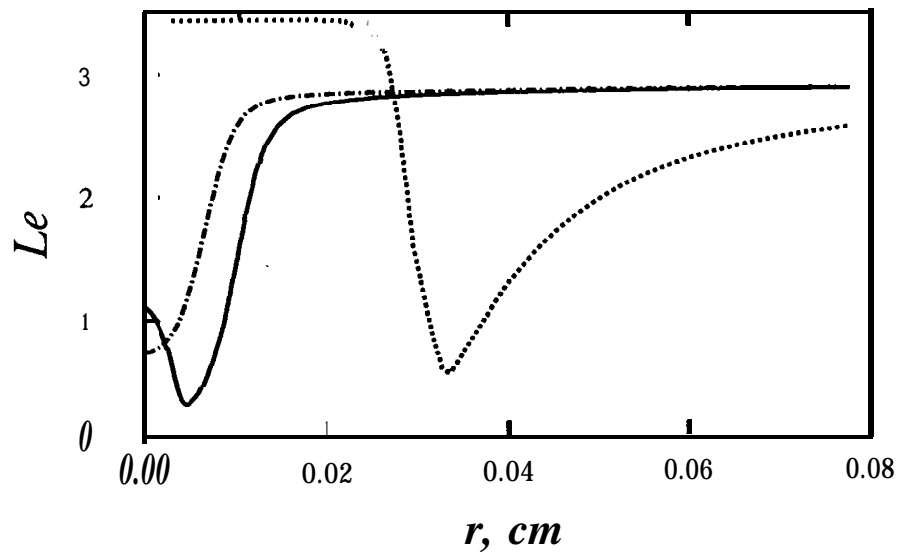


Fig 5a







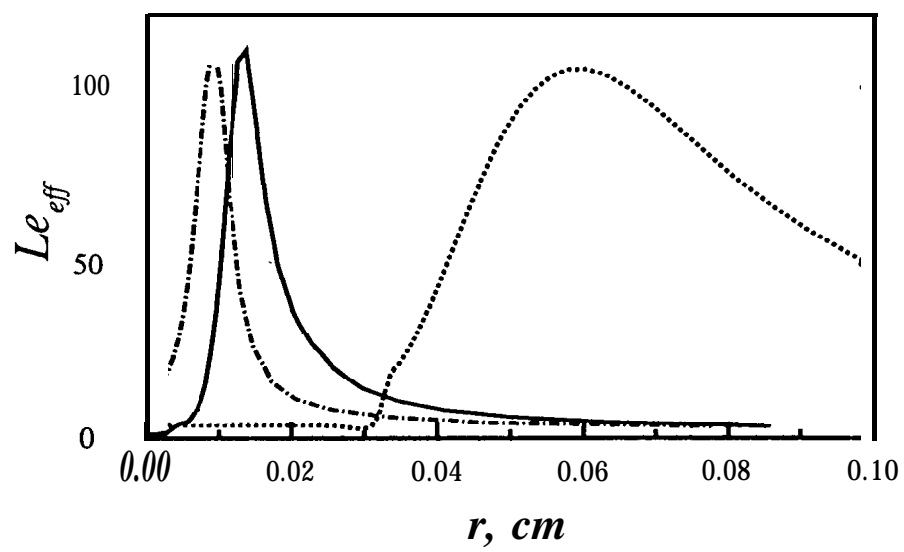
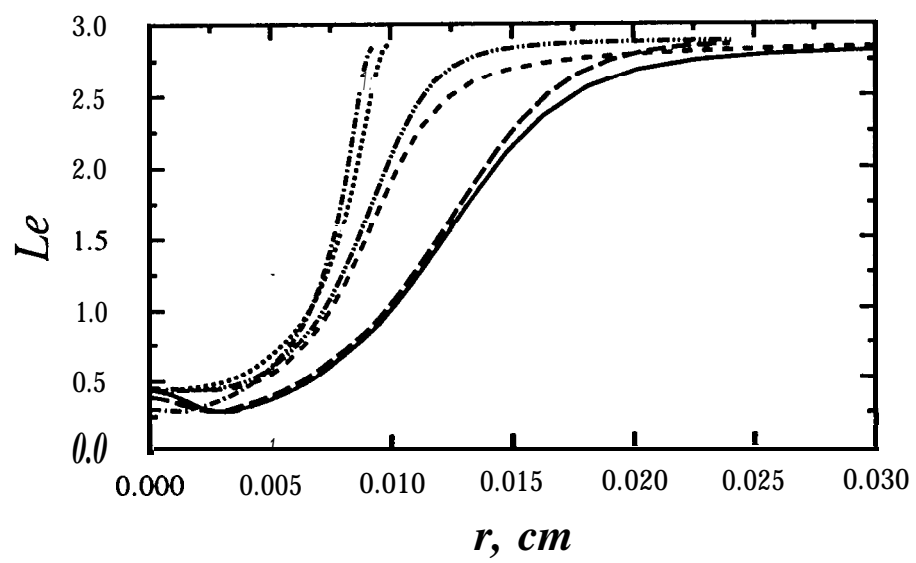


Fig 6 b



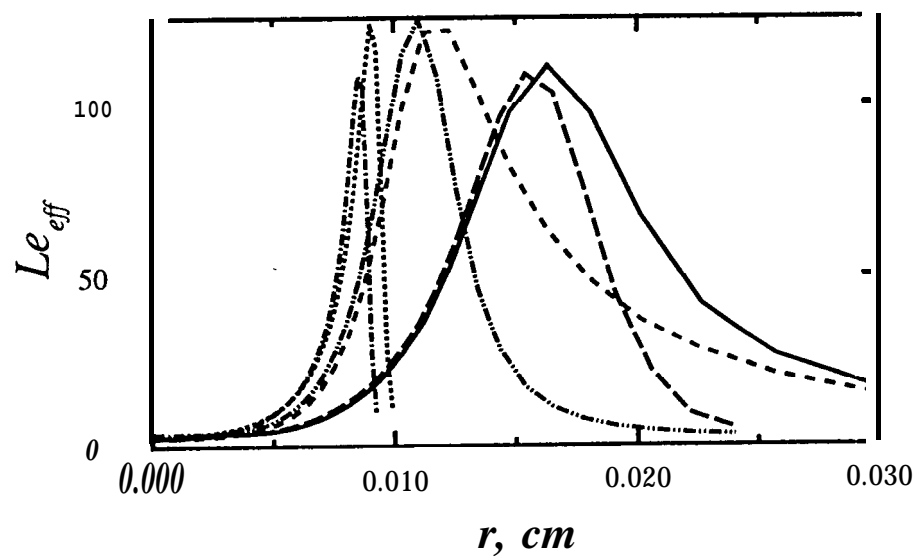


Fig 76

